ORGANIC LETTERS

2009
Vol. 11, No. 22
5114−5117

Guanosine + OH Radical Reaction in Aqueous Solution: A Reinterpretation of the UV−vis Data Based on Thermodynamic and Kinetic Calculations

Annia Galano*,† and J. Raul Alvarez-Idaboy*,‡

Departamento de Química, Universidad Autónoma Metropolitana-Iztapalapa, 09340 México D. F., México, and Facultad de Química, Departamento de Física y Química Teórica, Universidad Nacional Autónoma de México, México DF 04510, México

agalano@prodigy.net.mx; jidaboy@unam.mx

Received August 10, 2009

ABSTRACT

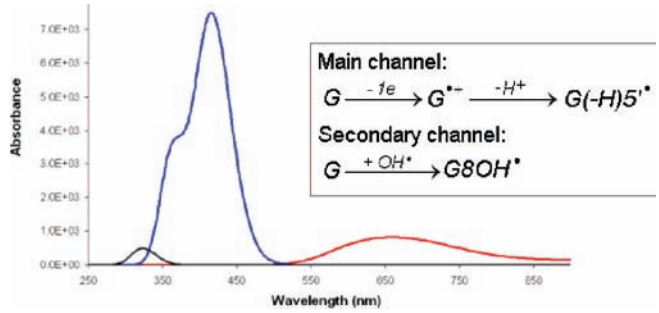

Thermodynamic and kinetic calculations have been used to reinterpret the UV−vis data related to the OH radical oxidation of guanosine. The main channel of reaction (70−75%) is proposed to be the formation of a guanosine radical cation followed by deprotonation. It accounts for both the absorbance decay at ∼620 nm and the build-up at ∼300 nm. A secondary channel yielding the G8OH adduct was found to contribute to the overall reaction by 12% at least.

Guanosine (G) is the most easily oxidized of the nucleic acid bases.[1] Its role as the predominant sink for hole transfer in double-stranded DNA has been justified by the fact that G has the lowest ionization potential among DNA components.[2] This explains why there are numerous chemical agents capable of abstracting one electron from G. Different values for the oxidation potential of G vs NHE have been reported: 1.29,[3] 1.16,[4] and 1.02 V.[5] Despite the variation among these values, they are all lower than the potential of the OH radical, 1.89 V,[6] and therefore this radical can act as a one-electron oxidizing agent when reacting with G.

Due to its importance for DNA damage processes, numerous studies have been devoted to the G + •OH reaction. In particular UV−vis spectral changes have been used to propose the most likely products and therefore the most probable mechanism of reaction. It has been observed that spectra taken at ∼1 μs after the pulse show characteristic bands at 300−310 nm, ∼400 nm, and ∼620 nm, while spectra taken at times ≥170 μs show a build-up of absor-

† Universidad Autónoma Metropolitana-Iztapalapa.
‡ Universidad Nacional Autónoma de México.

(1) Steenken, S. *Chem. Rev.* **1989**, *89*, 503, and references therein.
(2) Cadet, J.; Douki, T.; Ravanat, J.-L. *Acc. Chem. Res.* **2008**, *41*, 1075.
(3) Steenken, S.; Jovanovic, S. *J. Am. Chem. Soc.* **1997**, *119*, 617.
(4) Langmaier, J.; Samec, Z.; Samcova, E.; Hobza, P.; Reha, D. *J. Phys. Chem. B* **2004**, *108*, 15896.
(5) Xie, H.; Yang, D.; Heller, A.; Gao, Z. *Biophys. J.* **2007**, *92*, L70.
(6) Schwarz, H. A.; Dodson, R. W. *J. Phys. Chem.* **1984**, *88*, 3643.

10.1021/ol901862h CCC: $40.75
Published on Web 10/19/2009

bance for the first two bands and a decay for the latter one.[7,8] Candeias and Steenken[7] have assigned the ~620 nm band to adduct G4OH (Figure 1) and the 300−310 nm band to

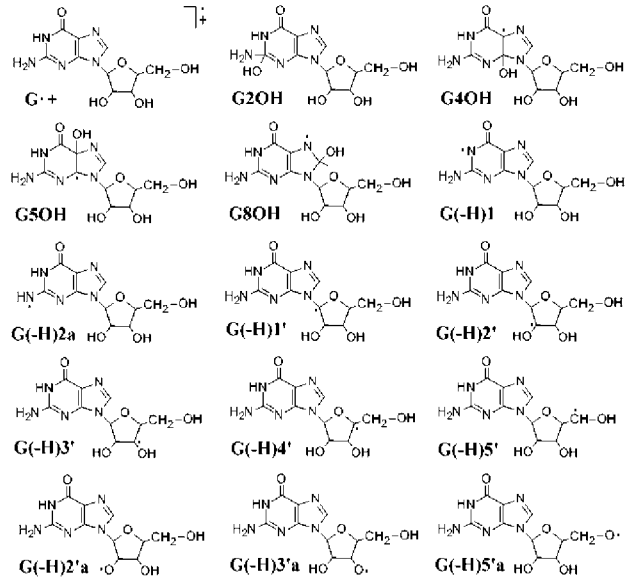

Figure 1. Studied products of the G + ·OH reaction.

the FaPyG[9] formation from G8OH. They also proposed that the yields, relative to OH, are 17% and 60−70% for G8OH and G4OH, respectively. Chatgilialoglu et al.,[8] on the other hand, assigned the broadband ~610 nm to the guanyl radical formed by H abstraction from the NH_2 moiety, G(−H)2a in Figure 1. These authors also proposed this abstraction path as the main channel of reaction and addition to C8 as a minor channel. Balasubramanian et al.[10] stated that OH damage to DNA strands is governed by the accessible surface areas of the H atoms in the DNA backbone. In particular, they found the 5′ site in deoxyribose as the most reactive one. In addition, the proton-coupled electron transfer mechanism has also been proposed by different authors.[11] In this case, the electron transfer is expected to be followed by the deprotonation of the radical cation ($G^{\bullet+}$), which has a pK_a = 3.9.[11a] Therefore, at physiological pH $G^{\bullet+}$ is expected to be found in one of its deprotonated forms, which also correspond to the H abstraction products: G(−H)·.

Therefore, since different hypotheses have been proposed, it is the main aim of the present work to identify the preponderant mechanism of the G + ·OH reaction. To that purpose, three different mechanisms have been taken into account.

Radical adduct formation (RAF):

$$G + {}^{\bullet}OH \rightarrow GOH^{\bullet} \qquad (I)$$

Hydrogen atom transfer (HAT):

$$G + {}^{\bullet}OH \rightarrow G(-H)^{\bullet} + H_2O \qquad (II)$$

Sequential electron proton transfer (SEPT):

$$G + {}^{\bullet}OH \rightarrow G^{\bullet+} + OH^{-} \qquad (IIIa)$$

$$G^{\bullet+} \rightarrow G(-H)^{\bullet} + H^{+} \qquad (IIIb)$$

For all the modeled species, full geometry optimizations and frequency calculations have been carried out using the M05-2X functional[12] and the 6-311++G(d,p) basis set. The stationary points were first modeled in the gas phase (vacuum), and solvent effects were included a posteriori by single-point calculations using a polarizable continuum model. The absorption spectra have been computed with time-dependent density functional theory (TDDFT) at the B3LYP/6-311++G(d,p) level of theory.

On the basis of the guanosine structure (Figure 2), four different channels of reaction have been modeled for the RAF

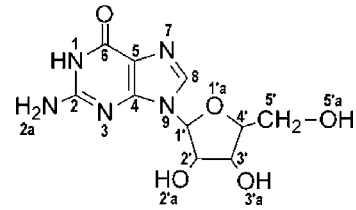

Figure 2. Guanosine.

mechanism, involving sites 2, 4, 5, and 8. For the HAT mechanism, H abstractions from sites 1 and 2a in the guanine moiety and from sites 1′, 2′, 3′, 4′, 5′, 2′a, 3′a, and 5′a in the ribose moiety have been considered. Deprotonations from all these sites have also been taken into account for the second step of the SEPT mechanism. Even though HAT from site 8 is not expected to compete with the other HAT paths of reaction studied in this work, we have calculated the ΔG of reaction for this path. It was found to be almost isoergonic, while the exergonicity of all the other computed HAT paths ranged from −11 to −28 kcal/mol. Accordingly, and based on the Bell−Evans−Polanyi principle, such a difference in ΔG means that the contributions of HAT from site 8 to the overall reaction are negligible. Therefore, it will not be considered any further.

(7) Candeias, L. P.; Steenken, S. *Chem.−Eur. J.* **2000**, *6*, 475.
(8) Chatgilialoglu, C.; D'Angelantonio, M.; Guerra, M.; Kaloudis, P.; Mulazzani, Q. G. *Angew. Chem., Int. Ed.* **2009**, *48*, 1.
(9) FapyG = 2,6-diamino-4-hydroxy-5-formamidopyrimidin.
(10) Balasubramanian, B.; Pogozelski, W. K.; Tullius, T. D. *Proc. Natl. Acad. Sci. U.S.A.* **1998**, *95*, 9738.
(11) Some examples are: (a) Steenken, S. *Chem. Rev.* **1989**, *89*, 503. (b) Neeley, W. L.; Essigmann, J. M. *Chem. Res. Toxicol.* **2006**, 19–491, and references therein. (c) Cadet, J.; Douki, T.; Ravanat, J.-L. *Acc. Chem. Res.* **2008**, *41*, 1075.
(12) Zhao, Y.; Schultz, N. E.; Truhlar, D. G. *J. Chem. Theory Comput.* **2006**, *2*, 364.

The UV−vis spectra for all the studied products of reaction (Figure 1) are provided as Supporting Information (Figure S1), as well as the details on the main optical transitions (Table S1, Supporting Information). The spectra have been computed within the continuous model, using gas-phase optimized geometries. This approach is based on the assumption that geometries would be very similar in both cases. However, to check the validity of such an assumption, the geometries of selected species were also optimized in solution, and their UV−vis spectra were recomputed. We have selected those structures more relevant to our study: the radical cation, G8OH, G(−H)5′, and G(−H)2a. As shown in Figure S2 (Supporting Information), the assumption is correct, and the spectra are very similar. The major difference is that the absorbance is systematically lower when geometries optimized in solution are used, but the position and the shape of the bands remain almost the same. Since the mechanistic elucidation is based on the wavelengths, the conclusions derived from the spectra analysis are the same for both approaches.

The computed UV−vis spectra show that four possible products of reaction significantly absorb in the 600−650 nm region: the radical cation formed in step a of SEPT and the HAT/deprotonation products G(−H)1, G(−H)2a, and G(−H)2′a. There are also several products of reaction that have significant absorbance in the 300−350 nm region: G(−H)1′, G(−H)2′, G(−H)3′, G(−H)5′, G5OH, and G8OH. Therefore, even when it is true that time-dependent DFT calculations provide reliable optical transition, as stated by Chatgilialoglu et al.,[8] they are not enough to support the identification of the most probable mechanism of reaction, i.e., the most abundant products. Accordingly, in the present work thermodynamic and kinetic calculations have been performed to help reinterpret the UV−vis data and to propose the most viable mechanism for the G + $^{\bullet}$OH aqueous reaction.

The electron transfer from G to $^{\bullet}$OH was found to be exergonic by 1.78 kcal/mol when the solvent is included only as a continuum model and by 2.98 kcal/mol when, in addition to the continuum, two water molecules are explicitly included. Therefore, independently of the model the IIIa step is energetically feasible, which is in agreement with the reported redox potentials. The Gibbs free energies of reaction (ΔG) corresponding to $^{\bullet}$OH addition and H abstraction processes are reported in Table S2 (Supporting Information). As these values show, all of them are exergonic, and with the exception of the G5OH and G(−H)1′ formation, the exergonicity is large enough to make the reversible reactions negligible. Therefore, kinetic criteria must be used to identify the main channel of reaction. The barriers of reaction in terms of Gibbs free energy are also reported in Table S2 (Supporting Information) for mechanisms I and II. The barrier for step IIIa was calculated as explained in the computational details (Supporting Information), and it was found to be equal to 2.68 kcal/mol. The overall rate constant, calculated as the sum of the rate constants for each channel of reaction, was found to be equal to 9.66×10^9 L mol^{-1} s^{-1}. The contributions from HAT, RAF, and SEPT mechanisms are 1.42%, 25.32%, and 73.26%, respectively. However, taking into account the average mean unsigned error reported for kinetic calculations performed with the M05-2x functional (1.4 kcal/mol[13]), we propose the following contributions: 1−5%, 24−25%, and 70−75% for HAT, RAF, and SEPT mechanisms, respectively. These variations are rather small because the main channels of reaction are diffusion controlled.

In addition to the continuum, two other solvation models have been tested, as suggested by the reviewers (Table S3, Supporting Information). One includes an explicit water molecule and excludes the continuum, and the other is a mixed model including both the continuum and an explicit water molecule. We have tested the influence of the different solvation approaches for three representative channels. They are SEPT and HAT from the 5′ site and RAF at the 8 site. As the results in Table S3 (Supporting Information) show, the values obtained within the continuum approach lie in between those obtained with the other two models. The inclusion of a water molecule excluding the continuum leads to the highest rate constants for HAT and RAF mechanisms, while the mixed model leads to the lowest ones. However, the SEPT mechanism is systematically predicted as the main channel of reaction, which is the main conclusion from this work. The best agreement with experiments is achived when using the contiunuum approach. Taking into account this comparison together with the ranges proposed by taking into account the average error of the used functional and the agreement with the experimental data, we are confident about the proposed branching ratios.

The proposed branching ratios for each possible channel of reaction are provided in Table S4 (Supporting Information). The formation of G8OH was found to contribute to the overall $^{\bullet}$OH consumption by 12.05%, which is in good agreement with the 17% proposed by Candeias and Steenken.[7] However, it should be noticed that our value might be underestimated due to the potential reversibility of G5OH formation. Since it is a unimolecular process, the G5OH decomposition yielding the starting reactants (G and $^{\bullet}$OH) might occur to a significant extent, which would increase the branching ratios of the other products.

According to our results, and in agreement with the redox potentials of G and $^{\bullet}$OH, the main channel of reaction is proposed to be the electron transfer from G to $^{\bullet}$OH, i.e., the one-electron oxidation of guanosine. Since it has been established that at physiological pH the G$^{\bullet+}$ is in one of its deprotonated forms, the Maxwell−Boltzmann distribution including all the deprotonation products has been computed (Table S5, Supporting Information). According to our results, 91.63% of the deprotonated guanosine radical cation exists as G(−H)5′. This result is in agreement with the findings of Balasubramanian et al.[10] for double-stranded DNA.

Analyzing all the above-discussed results together, we propose the following mechanism for the $^{\bullet}$OH oxidation of guanosine in aqueous solution at physiological pH.

(13) Zhao, Y. Schultz, N. E.; Truhlar, D. G. *J. Chem. Phys.* **2005**, *123*, 161103.

Main channel:

$$G \xrightarrow{-1e} G^{\bullet+} \xrightarrow{-H^+} G(-H)5'$$

Secondary channel:

$$G \xrightarrow{+OH^\bullet} G8OH^\bullet$$

The first step of G oxidation is the formation of the guanosine radical cation, which is in agreement with the mechanism previously proposed in ref 11b. Our proposal provides a viable explanation to the observed decay of the UV−vis band at ∼620 nm and the build-up of absorbance for the bands at ∼300 and ∼400 nm. According to the kinetic calculations, the fastest reaction is the electron transfer from G to •OH, which is also favored by the fact that the reaction distance needed for this process to occur is longer than for any of the HAT or RAF reactions. Therefore, at very short times of reaction the main product is expected to be $G^{\bullet+}$, which shows a broadband of absorption in the 500−650 nm region according to the experimental UV−vis spectra.[7,8] The computed spectrum of $G^{\bullet+}$ reproduces not only the position of the main optical transition (630 nm) but also the broad shape of the band. As the time of reaction increases, $G^{\bullet+}$ deprotonates causing the decay of this absorption band. The build-up of the band at ∼300 nm is then explained by the formation of the deprotonation product found as the most viable one, G(−H)5′ which, according to our calculations, shows the maximum absorption at 315 nm. Therefore, the deprotonation of the guanosine radical cation explains both the decay at ∼620 nm and the build-up at ∼300 nm. The band at ∼400 nm can be assigned at the addition products, particularly at the most probable one: G8OH that shows its maximum absorption at 410 nm (Table S1, Supporting Information). The build-up effect for this band, which is much less noticeable than the one at ∼300 nm,[7,8] might be attributed to the reversibility of the G5OH formation which in due time might increase the relative G8OH population. In fact, any reversible process is expected to contribute to such an increase since the G8OH product is the lowest in energy from all the studied ones (Table S2, Supporting Information).

Figure 3 summarizes our reinterpretation of the UV−vis spectra, according to the computed thermodynamic and kinetic data. The finding that G8OH shows a much higher absorbance than $G^{\bullet+}$ and G(−H)5′ while the experimental spectra do not show the higher absorbance in this region also supports that G8OH is a minor product that should be in much lower concentrations than $G^{\bullet+}$ and G(−H)5′, which are the species involved in the proposed main channel of reaction.

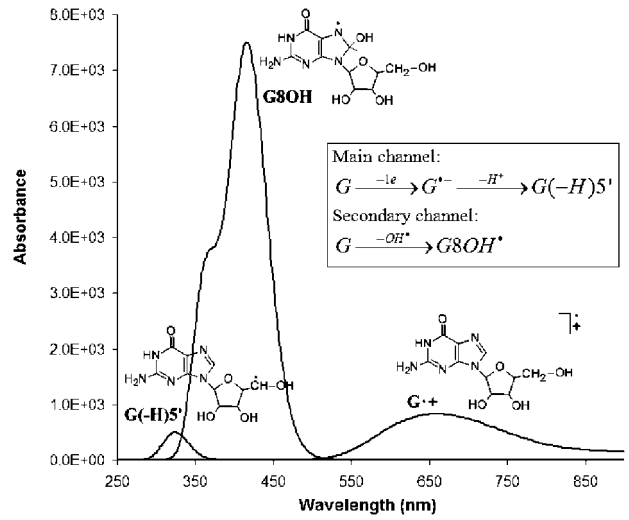

Figure 3. UV−vis spectra interpretation and mechanism for the •OH oxidation of guanosine.

Acknowledgment. A.G. thanks Laboratorio de Visualización y Cómputo Paralelo at UAM - Iztapalapa for the access to its computer facilities. J. R. A.-I. thanks the Dirección General de Servicios de Cómputo Académico (DGSCA) at Universidad Nacional Autónoma de México. This work was partially supported by a grant from the DGAPA UNAM (PAPIIT- IN203808).

Supporting Information Available: Computational details; UV−vis spectra of all the studied products; details on the main vertical optical transitions; coordinates of selected transition states; Gibbs free energies of reaction; branching ratios; and Maxwell−Boltzmann distribution of deprotonation products. This material is available free of charge via the Internet at http://pubs.acs.org.

OL901862H